LONDON
SCHOOL of
HYGIENE
&TROPICAL
MEDICINE

Boonyalai, Nonlawat; Collins, Christine; Hackett, Fiona; Withers-Martinez, Chrislaine; Blackman, Michael (2018) Function and essentiality of Plasmodium falciparum Plasmepsin V. BioRxiv. DOI: https://doi.org/10.1101/404798

Function and essentiality of *Plasmodium falciparum* plasmepsin V

Nonlawat Boonyalai[1,a] *, Christine R. Collins[2], Fiona Hackett[2], Chrislaine Withers-Martinez[2], and Michael J. Blackman[2,3]*

[1] Department of Biochemistry, Faculty of Science, Kasetsart University, Chatuchak, Bangkok 10900, Thailand.

[2] Malaria Biochemistry Laboratory, The Francis Crick Institute, London NW1 1AT, UK

[3] Department of Pathogen Molecular Biology, London School of Hygiene & Tropical Medicine, London WC1E 7HT, UK

[a] Present address: Department of Immunology and Medicine, US Army Medical Directorate-Armed Forces Research Institute of Medical Science (USAMD-AFRIMS), Bangkok, Thailand.

*Correspondence and requests for materials should be addressed to N.B.(nonlawat.b@ku.ac.th or nonlawatb.ca@afrims.org) and M.J.B (mike.blackman@crick.ac.uk)

Running title: *Plasmodium falciparum* plasmepsin V is essential for parasite viability

Abstract

The malaria parasite replicates within erythrocytes. The pathogenesis of clinical malaria is in large part due to the capacity of the parasite to remodel its host cell. To do this, intraerythrocytic stages of *Plasmodium falciparum* export more than 300 proteins that dramatically alter the morphology of the infected erythrocyte as well as its mechanical and adhesive properties. *P. falciparum* plasmepsin V (PfPMV) is an aspartic protease that processes proteins for export into the host erythrocyte and is thought to play a key role in parasite virulence and survival. However, although standard techniques for gene disruption as well as conditional protein knockdown have been previously attempted with the *pfpmv* gene, complete gene removal or knockdown was not achieved so direct genetic proof that PMV is an essential protein has not yet been established. Here we have used a conditional gene excision approach combining CRISPR-Cas9 gene editing and DiCre-mediated recombination to functionally inactivate the *pfpmv* gene. The resulting mutant parasites displayed a severe growth defect. Detailed phenotypic analysis showed that development of the mutant parasites was arrested at the ring-to-trophozoite transition in the erythrocytic cycle following gene excision, likely due to a defect in protein export. Our findings are the first to elucidate the effects of PMV gene disruption, showing that it is essential for parasite viability in asexual blood stages. The mutant parasites can now be used as a platform to further dissect the *Plasmodium* protein export pathway.

Introduction

Malaria was responsible for approximately 445,000 deaths and 216 million clinical cases in 2016, an increase of ~5 million cases over the previous year [1]. Vital to the growth and pathogenicity of the parasite is host cell remodelling in which the parasite modifies the host erythrocyte by the synthesis and export of over 300 parasite proteins beyond the bounds of the parasitophorous vacuole (PV) within which it replicates (for reviews, see [2,3]). The exported proteins are trafficked from the parasite to the host erythrocyte via a putative parasite-derived protein complex known as the translocon of exported proteins (PTEX), located within the PV membrane (PVM) [4,5]. The exported proteins extensively alter the mechanical and adhesive properties of infected erythrocytes, resulting in vascular sequestration of the infected cells and eventual destruction of the host erythrocyte [6]. Protein export in *Plasmodium* has been most intensively studied in *P. falciparum* (reviewed in [7,8]), where the majority of known exported proteins contain the pentameric localisation motif RxLxE/Q/D, termed *Plasmodium* export element (PEXEL), typically located downstream of the N-terminal secretory signal sequence that regulates entry into the ER [9,10]. Some proteins lacking a PEXEL motif, referred to as PEXEL-negative exported proteins (PNEPs), can also be exported [11]. PNEPs do not contain a typical secretory signal sequence so are unlikely to be N-terminally processed , but the first 20 amino acid residues of PNEPs are sufficient to mediate their export. The unfolding of soluble PNEPs is then required for trafficking into the host cell [12].

P. falciparum plasmepsin V (PfPMV) is an ER-located aspartic protease comprising 590 amino acid residues (~68 kDa) [13]. PfPMV expression levels in the parasite progressively increase throughout schizogony [13]. Numerous studies have now established that PMV is directly responsible for cleavage of the PEXEL motif within exported proteins. Cleavage occurs on the C-terminal side of the conserved Leu residue (RxL↓), revealing a new N-terminus that is rapidly acetylated (^{Ac}-xE/Q/D) [14]. A recent x-ray

70   crystal structure of *Plasmodium vivax* PMV (PvPMV) revealed a canonical aspartyl protease fold with

71   several important features [15]. These include a nepenthesin (NAP)-like insertion within the N-terminal

72   part of the enzyme, which may control substrate entry into the active site and influence enzyme

73   specificity, as well as a helix-turn-helix (HTH) motif near the C-terminus of the enzyme, which is

74   conserved in PMV from other *Plasmodium* species but not found in other parasite plasmepsins involved

75   in haemoglobin digestion. PMV also possesses an unpaired Cys residue (C140 in PvPMV, equivalent to

76   C178 in the *P. falciparum* enzyme) which is located in the flap of the structure and is restricted to

77   *Plasmodium* species. In attempts to establish the druggability and function of PMV, several

78   peptidomimetic inhibitors based on the PEXEL motif have been developed [16-18]. A co-crystal structure

79   of PMV bound to one of these compounds, the PEXEL-mimetic WEHI-842, showed that although the

80   unpaired Cys points into the active site of the enzyme, it does not appear to make contact with the

81   inhibitor [15,19]. Another inhibitor, WEHI-916, inhibits the activity of purified PMV isolated from both

82   *P. falciparum* and *P. vivax*, and higher concentrations of WEHI-916 were required to kill parasites

83   engineered to over-express PfPMV indicating on-target efficacy [16,18]. Compound 1, a hydroxyl-

84   ethylamine PEXEL-mimetic, inhibited PfPMV activity in vitro with picomolar potency but failed to

85   block parasite growth due to poor stability and membrane permeability [17]. Collectively, these findings

86   indicate that PMV has a number of distinguishing features that could be exploited in drug design, and can

87   potentially be targeted with suitable inhibitory compounds.

88   An important component in the validation of any enzyme as a drug target is genetic ablation of

89   enzyme expression. Unfortunately, previous attempts to genetically delete or knock-down PMV

90   expression have been only partially successful. Work by Boddey et al [20] failed to disrupt the *P. berghei*

91   PMV (PbPMV), suggesting (but not proving) that the gene is essential. Russo et al [21] similarly

92   attempted to disrupt the *pfpmv* gene using an allelic replacement approach. Single crossover homologous

4

93   recombination into the endogenous PMV locus was possible only when the catalytic dyad aspartate codon

94   was preserved, whilst four separate transfection experiments with constructs designed for non-

95   synonymous alteration of the active site codon were not successful. Conditional knockdown of PfPMV

96   expression was also attempted using the RNA-degrading *glmS* ribozyme system [18]. Although this

97   resulted in around 75-90% knockdown of PMV expression, the remaining PMV levels were presumably

98   sufficient to enable export and sustain parasite development. Gambini et al [17] generated an inducible

99   PMV knock-down by fusing PMV with a destabilising domain (DD), but only a 4 to 10-fold knock-down

100   of PMV cellular levels was achieved using this approach, which did not affect parasite viability. In

101   summary, whilst some of these data are consistent with an essential role for PMV, in the absence of any

102   reports of complete ablation of PfPMV expression, direct genetic proof that PMV is an essential protein is

103   lacking.

104   Here we have used a robust conditional genetic approach to truncate the *pfpmv* gene. Our findings

105   are the first to confirm genetically that deletion of PfPMV has a significant effect on ring-to-trophozoite

106   development and ultimately results in parasite death.

107

Results

Generation of modified *pfpmv* parasites using CRISPR-Cas9

Previous attempts to disrupt the *pfpmv* gene using conventional genetic techniques were unsuccessful [20,21], and conditional knockdown approaches did not significantly affect PEXEL processing or parasite viability [17,18], presumably due to relatively low levels of PfPMV expression being sufficient to sustain parasite viability. To explore the consequences of complete functional inactivation of PMV, we therefore took advantage of the DiCre conditional recombinase system, recently adapted to *P. falciparum* [22]. Using Cas9-mediated genome editing [23] we first introduced synthetic introns containing *loxP* sites [24] into the endogenous *pfpmv* locus such that they flanked (floxed) an internal segment of the gene encoding Asp133 to Thr590. At the same time, the modified gene was fused to a C-terminal HA3 epitope tag, as well as a 2A sequence followed by the aminoglycoside 3'-phosphotransferase (*neo-R*) gene sequence conferring neomycin resistance activity to enable selection for integration events (Fig 1A). Importantly, one of the PfPMV catalytic dyad residues (Asp365) is included within the floxed region. The repair plasmid pT2A-5´UTR-3´-PMV- ΔDHFR was based on pT2A-DDI-1cKO, which contains a modified selection-linked integration (SLI) region [25]. The genomic modification was made in the DiCre-expressing *P. falciparum* B11 parasite clone [26] such that excision of the floxed sequence could be induced by treatment of the transgenic parasites with rapamycin (RAP). DiCre-mediated excision was predicted to generate an internally-truncated mutant form of PMV lacking one of the catalytic dyad residues. Excision would also remove the *neo-R* gene and induce expression of GFP as a fluorescence reporter indicative of parasites expressing the truncated *pfpmv* gene (Fig 2A).

Fig 1. Generation of *P. falciparum* parasite lines expressing PfPMV-HA. (A) Using Cas9-mediated recombination, the region of the *pfpmv* gene encoding Asp133 to Thr590 was replaced with two *loxP* (black arrowhead)-containing *P. falciparum* SERA2 introns (yellow box) flanking a recondonised *pfpmv* (blue box) fused to a *3xHA* epitope tag (purple box), a *2A* sequence (pink box), and a *neo-R* gene (white box) and stop codon (red hexagon). The second *loxPint* was also fused with *2A* and *gfp* gene sequences. The *gfp* gene is translated only following site-specific recombination of the *loxP* sites by DiCre recombinase. Positions of hybridisation of primers used for confirmation of the integration event by diagnostic PCR are shown as coloured arrows. (B) Diagnostic PCR analysis of genomic DNA of the control parental B11 and integrant *P. falciparum* clones, confirming the predicted homologous recombination event.

Fig 2. DiCre-mediated conditional disruption of *P. falciparum* PMV expression. (A) Strategy for conditional truncation of the *pfpmv* gene. Positions of hybridisation of primers used for diagnostic PCR analysis of the integration and excision events are shown as coloured arrows. (B) Diagnostic PCR analysis of genomic DNA from transgenic *P. falciparum* PMV-C5 line at 24 h in cycle 0 (~20 h post RAP- or DMSO-treatment), confirming the predicted DiCre-mediated excision events. Expected sizes of the PCR amplicons specific for the intact or excised locus are indicated. (C) Live GFP fluorescence assay of cycle 0 PMV-C5 parasites ~42 h following treatment at ring stage with DMSO or RAP. Parasite nuclei were stained with Hoechst 33342. (D) Giemsa-stained blood smears, showing the morphology of treated PMV-C5 parasites. The time-course of treatment and subsequent monitoring of the cultures is indicated (top).

7

154

155   Successful modification of the *pfpmv* gene in the transfected parasite population following the

156   introduction of the targeting vector was confirmed by diagnostic PCR (data not shown). Limiting dilution

157   cloning of the modified parasites resulted in the isolation of parasite clones PMV-C5 and PMV-F9, which

158   were derived from independent transfections using different guide RNAs. Modification of the native

159   *pfpmv* locus was confirmed in both transgenic parasite lines by diagnostic PCR (Fig 1B). Both clones

160   replicated at a rate indistinguishable from that of the parental B11 parasites, suggesting that the

161   modifications did not affect parasite viability. Transgenic parasite clone PMV-C5 was used for all

162   subsequent experiments.

163

164 **Conditional truncation of the *pfpmv* gene leads to a developmental arrest**

165   Expression of the recodonised *pfpmv* gene in transgenic parasite clone PMV-C5 was expected to

166   produce an epitope-tagged PMV product (called PMV-HA), as well as expression of the *neo-R* gene

167   product. Note that in this event GFP is not produced because of the presence of a translational stop codon

168   directly downstream of the *neo-R* gene. Upon RAP-treatment, site-specific recombination between the

169   introduced *loxP* sites in the modified *pfpmv* locus of the PMV-C5 parasites was anticipated to reconstitute

170   a functional, albeit chimeric, intron. Splicing of this chimeric intron results in a truncated form of PMV

171   lacking the HA epitope tag, as well as allowing expression of free GFP. DNA extracts of RAP-treated and

172   mock-treated (DMSO-treated control) PMV-C5 parasites were analysed by diagnostic PCR (Fig 2A). To

173   confirm whether RAP-induced DiCre-mediated excision took place as expected, we monitored the

174   appearance of GFP-positive parasites following treatment of synchronous ring-stage parasites with

175   DMSO or RAP. As expected, GFP fluorescence was only detected in the RAP-treated parasites (Fig 2C).

176   Indeed, no parasites lacking GFP fluorescence could be detected upon microscopic examination of the

8

177   RAP-treated cultures, indicating highly efficient excision of the floxed *pfpmv* sequence. This was

178   confirmed by FACS analysis (Fig 3B), showing that 98.86 % of the RAP-treated parasites displayed GFP

179   fluorescence. These results confirmed the PCR-derived excision data and demonstrated essentially

180   complete conditional truncation of PMV within a single erythrocytic cycle in the PMV-C5 parasite clone.

181

182   **Fig 3. Functional disruption of PfPMV results in developmental arrest at the ring-to-trophozoite**

183   **transition.** (A) Growth assay showing relative replication rates over the two erythrocytic cycles

184   following treatment of PMV-C5 ring stages with DMSO or RAP. Parasite number values were

185   determined by FACS as described in Materials and Methods. (B) GFP fluorescence at ~42 h (schizonts)

186   of the PMV-C5 line treated at ring stage with DMSO (black) or RAP (green) as determined by flow

187   cytometry of fixed cultures. The percentage of GFP-positive RAP-treated parasites (i.e. the excision rate)

188   was 98.86%. (C) Western blot analysis of clone PMV-C5 following mock-treatment (-RAP) or RAP-

189   treatment (+RAP). Schizont extracts (~42 h post-treatment) were probed with antibodies to detect HA-

190   tagged PfPMV (anti-HA), or antibodies to GFP, MSP1, KAHRP, or HRP2.

191

192   To initially explore the effects of PMV truncation on parasite viability, we examined growth and

193   development of the ΔPMV mutant by microscopic examination of Giemsa-stained cultures. This revealed

194   that although RAP-treated PMV-C5 parasites appeared morphologically normal throughout the

195   erythrocytic growth cycle in which the parasites were treated (henceforward referred to as cycle 0),

196   development of the mutant parasites stalled at ring stage in the following cycle (cycle 1; Fig 2D). By the

197   end of cycle 1, only arrested pycnotic forms were observed. Collectively, these results suggested that

198   ablation of PMV expression causes a severe growth defect and developmental arrest between ring and

199   trophozoite stage.

200

Egress, Invasion and Protein export are not affected by disruption of the *pfpmv* gene in cycle 0

203   Whilst the above results showed that truncation of PfPMV affected parasite development in cycle

204 1, it did not rule out the possibility of defects in egress and invasion of fresh erythrocytes at the end of

205 cycle 0 (the cycle of RAP-treatment). To evaluate and quantify this, we used flow cytometry to monitor

206 increases in parasitaemia at the transition between cycle 0 schizonts and cycle 1 rings. As shown in Fig

207 3A, the parasitaemia of PMV-C5 cultures at the end of cycle 0 as well as at the early ring stage of cycle 1

208 was unaffected by RAP-treatment, indicating no effects of PMV ablation on schizont development in

209 cycle 0, or the egress and invasion capacity of the released merozoites. However, upon further

210 development of the new parasite generation in cycle 1, the parasitaemia in the RAP-treated culture

211 reached plateau after the ring-trophozoite transition. This confirmed that the truncation of PfPMV did not

212 cause any effects on egress and invasion and that the enzyme is essential for the ring to trophozoite

213 developmental transition of the intracellular parasite. Confirmation of the high excision rate of the PMV-

214 C5 clone following RAP-treatment was also confirmed by FACS analysis (Fig 3B).

215   To further explore the PMV-null phenotype, we examined the expression of PMV-HA as well as

216 other non-exported and exported parasite proteins. Extracts of DMSO and RAP-treated PMV-C5

217 parasites were analysed by immunoblot ~42 h following treatment, using antibodies specific for the HA

218 epitope tag as well as GFP, the merozoite plasma membrane surface protein MSP1, and the exported

219 proteins KAHRP and HRP2. As shown in Fig 3C, only a faint HA signal was detected in the RAP-treated

220 sample, whilst a corrrespondingly strong GFP signal was observed only in this sample. These data were

221 in good agreement with the diagnostic PCR results, indicating high efficiency of conditional excision of

222 the floxed sequence in the PMV-C5 clone. In contrast, no differences between DMSO- and RAP-treated

223 parasites were detectable in expression levels of MSP1 (thought to play an important role in egress and

224 invasion [27]) Similarly, there were no significant differences in expression of KAHRP and HRP2, both

225 of which are examples of PEXEL-containing proteins that are cleaved by PMV [20,21,28]. This is

226 consistent with the notion that protein export remains unaffected in cycle 0 in the RAP-treated parasites.

227 We next determined the effects of PfPMV truncation on its subcellular localisation within the

228 parasite, as well as on the trafficking of other exported proteins in cycle 0. Immunofluorescence analysis

229 (IFA) showed that, as expected, PMV-HA showed a perinuclear localisation in schizonts of control PMV-

230 C5 parasites but the signal was lost in RAP-treated parasites (Fig 4). To determine the effects of PMV

231 ablation on protein export, mock- and RAP-treated PMV-C5 parasites were probed with anti-KAHRP2

232 and anti-HRP2 antibodies. The localisation and intensity of the MSP1 signal and the KHARP signal did

233 not alter upon RAP-treatment, correlating well with the western blot analysis. The HRP2 signal remained

234 detectable in both control and the RAP-treated parasites, but in contrast to the situation with the other

235 proteins examined, the fluorescence intensity of the HRP2 signal was substantially decreased in RAP-

236 treated parasites, suggesting a partial effect of PMV depletion on HRP2 trafficking. Together, these data

237 confirmed the loss of PMV-HA in RAP-treated parasites whilst indicating that both exported proteins

238 (KAHRP and HRP2) and merozoite surface proteins still localise correctly in cycle 0. However, the

239 decreased HRP2 signal intensity was consistent with a partial impact on protein export in cycle 0.

240

241 **Fig 4. IFA of schizonts of control (DMSO-treated) and RAP-treated integrant clone PMV-C5 ~42 h**

242 **following treatment (cycle 0)**. The PMV-HA signal was lost following RAP treatment. Localization of

243 MSP1, KAHRP and HRP2 was unaffected; however, the HRP2 signal was significantly decreased in

244 intensity. Parasite nuclei were visualised by staining with DAPI.

245

Discussion

Malarial proteolytic enzymes play regulatory and effector roles in multiple key biological processes in this important pathogen and have long been of interest as potential drug targets. In this study, we have shown for the first time that functional ablation of the *pfpmv* gene leads to a block at the ring-to-trophozoite transition and death of the parasite. To achieve this, we employed the robust conditional DiCre approach in combination with Cas9-induced gene modification. This system provides a rapid and efficient means of generating transgenic parasites as well as enabling complete disruption of the gene of interest [29,30]. Our study demonstrates that DiCre-mediated conditional knockout is a powerful tool to study essential genes in the human malaria parasite. Our genetic strategy also incorporated a method to permit the selection of parasites in which genomic integration of the input constructs had taken place, termed selection-linked integration (SLI), previously developed by Birnbaum *et al* [25]. For this, our rescue plasmid contained an SLI-resistance marker (neomycin phosphotransferase), which was linked to the modified *pfpmv* gene separated by a 2A 'skip' peptide [31,32]. This approach allows selection for correct integration by one to two weeks of neomycin selection. In our case, with the assistance of Cas9-mediated integration we in fact did not need to use neomycin selection in our experiments to select for correct integration. However, our plasmids could be useful for future genetic complementation studies.

When the PMV-modified parasite clone PMV-C5 was RAP-treated at early ring stage for just 3 h, followed by removal of RAP, parasite development proceeded normally in the first erythrocytic cycle (cycle 0). Whilst expression of most of the parasite proteins examined appeared unaffected, we did observe some impact on expression of the exported parasite protein HRP2. This is reminiscent of the observation by Russo et al [21] that the levels of HRP2 and RESA (ring-infected erythrocyte surface antigen) were reduced by 30-50% in PMV mutants. We suspect that this may be due to low levels of PMV expression early in cycle 0, perhaps due to transcription early in the erythrocytic cycle prior to gene

269   excision. That low levels of PMV are sufficient to sustain development has also been indicated by

270   previous conditional protein knockdown experiments [18]. Egress and invasion at the end of cycle 0 was

271   not affected in the RAP-treated PMV-C5 parasites; however, parasite development in the next cycle

272   stalled at the ring-to-trophozoite transition. This phenotype is very similar to that observed upon

273   treatment with the PMV inhibitor WEHI-916 [18], where the drug-treated parasites showed a growth

274   defect at the ring-to-trophozoite transition from approximately 20 h post-invasion. A similar parasite

275   developmental arrest at ring stage was also observed following conditional ablation of the PTEX

276   component HSP101 [33,34]. This implies that PMV function may be associated with PTEX, and may be

277   essential for ring-to-trophozoite development.

278   In summary, using a DiCre-mediated conditional gene editing approach to selectively disrupt the

279   *pfpmv* gene, we have shown that the gene is essential for the ring-to-trophozoite transition of intracellular

280   growth. This engineered platform will be useful for further study of PEXEL-protein export as well as for

281   dissection of PMV domain interactions, providing further impetus for focusing on PMV as a new

282   potential antimalarial drug target.

283

284

Materials and Methods

P. falciparum culture, transfection and limiting dilution cloning

Parasites (wild type clone 3D7 and the DiCre-expressing clone B11 [26]) were routinely cultured at 37ºC in human erythrocytes at 1-4% haematocrit in RPMI 1640 (Life Technologies) supplemented with 2.3 gL^{-1} sodium bicarbonate, 4 gL^{-1} dextrose, 5.957 gL^{-1} HEPES, 0.05 gL^{-1} hypoxanthine, 0.5% (w/v) Albumax II, 0.025 gL^{-1} gentamycin sulphate, and 0.292 gL^{-1} L-glutamine (complete medium) in an atmosphere of 90% nitrogen, 5% carbon dioxide and 5% oxygen [35,36]. Routine microscopic examination of parasite growth was performed by fixing air-dried thin blood films with 100% methanol before staining with 10% Giemsa stain (VWR international) in 6.7 mM phosphate buffer, pH 7.1. For synchronization, mature schizont stage parasites were isolated on cushions of 70% (v/v) isotonic Percoll (GE Healthcare) as previously described [37,38]. Enrichment for ring stages following invasion was performed using 5% (w/v) D-sorbitol [38,39].

Cloning of repair plasmid pT2A-5´UTR-3´-PMV- ΔDHFR

pT2A-5´UTR-3´-PMV- ΔDHFR plasmid is based on vector pT2A-DDI-1cKO (a kind gift of Dr. Edgar Deu, the Francis Crick Institute). The plasmid comprised 5´UTR of *pfpmv* and nucleotides 1-397 of *pfpmv* (Met1 to Lys132), followed by synthetic heterologous *loxP*-containing *sera2* and *sub2* introns (*loxPint*) [24] flanking recodonised *pfpmv* sequence encoding residues Asp133 to Thr590 (GeneArt) fused to a 3xHA epitope tag sequence, a 2A 'skip' peptide (2A) [40], and the neomycin resistance gene (*neo*). The second *loxPint* site was immediately followed by another 2A sequence, a *gfp* gene and nucleotides 1333 to 1773 of *pfpmv* which encode Lys445 to Thr590, as a 3´- targeting sequence.

14

307 Overlapping PCR was used to generate the *loxPint*-2A-*gfp* fragment from the template pT2A-DDI-1-

308 cKO-complement (obtained from Dr. Edgar Deu, the Francis Crick Institute). The resulting PCR product

309 was digested with *Xho*I and ligated into pT2A-DDI-1cKO pre-digested with the same restriction

310 enzymes, yielding plasmid pT2A-DDI-1-cKO-modified GFP (S1 Fig). The 5´-targeting sequence (903

311 bp) was PCR amplified from 3D7 genomic DNA using Phusion HF DNA polymerase (NEB) with

312 forward primer P3.1-*Bgl*II_5´UTR_F-mod and reverse primer P2-Int_PMV_R. The recodonised fragment

313 (1,602 bp) containing *loxPint*, recondonised *pfpmv*, 3xHA, and 2A was amplified from the plasmid

314 17ACRILIP_2177297_endoPMV (GeneArt) with primers P4-PMV_int_F and P5-T2A_HA_R. PCR

315 products of 5´-target region and the recodonised fragment were ligated with pT2A-DDI-1-cKO-modified

316 GFP pre-digested with *Bgl*II and *Sal*I using In-fusion® HD cloning kit (Clontech, Mountain View, CA),

317 producing the plasmid pT2A-5´UTR-PMV-cKO. The 3´-target region (441 bp) was amplified from 3D7

318 genomic DNA using Phusion HF DNA polymerase (NEB) with forward primer P16-EcoRV-PMV-F and

319 reverse primer P17-EcoRV-PMV-R. This fragment was then ligated into pT2A-5´UTR-PMV-cKO pre-

320 digested with *Eco*RV, yielding the plasmid pT2A-5´UTR-3´PMV-cKO. The *hdhfr* gene was removed

321 from pT2A-5´UTR-3´PMV-cKO by digesting the plasmid with *Bam*HI and *Eco*RI. The plasmid

322 backbone was blunt-end using T4 DNA polymerase (NEB) then religated using T4 DNA ligase (NEB),

323 giving rise to the repair plasmid pT2A-5´UTR-3´-PMV- ΔDHFR.

324

Insertion of guide RNA sequences into CRISPR/Cas9 plasmids

326 Potential guide RNA sequences specifically targeting *pfpmv* were identified using Benchling

327 (https://benchling.com/crispr). Two sets of guide RNA sequences were selected. Two pairs of

328 complementary oligonucleotides (P18-sgPMV-1F and P19-sgPMV-1R; P20-sgPMV-2F, and P21-

329 sgPMV-2R) corresponding to the 19 nucleotides adjacent to the identified PAM sequences were

15

330   phosphorylated using T4 polynucleotide kinase, annealed and ligated into pL-AJP_004 [41] predigested

331   with *Bbs*I, resulting in the two guide vectors pSgRNA1 and pSgRNA2.

332

Generation of *pmv-loxPint* parasites and conditional PMV truncation

334   The repair plasmid pT2A-5´UTR-3´-PMV- ΔDHFR was linearized with *Sca*I prior to

335   electroporation. Percoll-enriched mature schizonts of *P. falciparum* clone B11 were electroporated with

336   20 µg of pSgRNA1 or pSgRNA2 and 60 µg of linearized pT2A-5´UTR-3´-PMV- ΔDHFR using an

337   Amaxa P3 primary cell 4D Nucleofector X Kit L (Lonza) as described [22]. Twenty-four hours post-

338   transfection, the electroporated parasites were treated with 2.5 nM WR99210 for 96 h to select for

339   transfectants harbouring pSgRNA plasmids before returning the cultures to medium without drug.

340   Integrant parasites generally reached parasitaemia levels suitable for cryopreservation within 2-5 weeks.

341   Detection of the *pfpmv*-loxPint modified locus was carried out by diagnostic PCR using primer pairs P6-

342   5´UTR_Screen_F and P23-rcPMV-5´integr-R, P6-5´UTR_Screen_F and 198_GFP_start_seq_R, and P24-

343   GFP-3´integr-F and P25-3´UTR-PMV-R. The wild-type *pfpmv* locus was detected by diagnostic PCR

344   using primers P6-5´UTR_Screen_F and P22-PMV-endo-R. Transgenic parasite clones were obtained by

345   limiting dilution cloning by plating a calculated 0.3 parasite per well in flat-bottomed 96-well microplate

346   wells as described [42]. Wells containing single plaques were subsequently expanded into round-

347   bottomed wells. Transgenic parasite clones (PMV-C5 and PMV-F9) were finally checked by diagnostic

348   PCR for integration and modification of the endogenous *pfpmv* gene. Once established, all transgenic

349   clones were maintained in medium without any drug.

350   Recombination between the *loxPint* sites was induced in tightly synchronised ring-stages of

351   parasite clone PMV-C5 by incubation for 3 h in the presence of 100 nM RAP in 1% (v/v) DMSO; mock

352   treatment was with 1% (v/v) DMSO only. DiCre-mediated excision of the floxed *pfpmv* was detected by

16

353   PCR analysis of parasite genomic DNA using primers P6-5´UTR_Screen_F and P23-rcPMV-5´integr-R,

354   and P6-5´UTR_Screen_F and Deu198_GFP_start_seq_R. Truncation of *Pf*PMV was evaluated by

355   immunoblot analysis of SDS extracts of mature Percoll-enriched schizonts, probing with the anti-HA

356   antibody 3F10 (Roche), followed by horseradish peroxidase-conjugated secondary antibodies.

357

Nucleic acid extraction and polymerase chain reaction

359   For DNA extraction, total cell pellets were first treated with 0.15% saponin in PBS for 10 min,

360   then washed with PBS before DNA was extracted using a DNeasy® Blood & Tissue Kit (QIAGEN). For

361   diagnostic PCR amplification, GoTaq® (Promega) DNA master mix was used. Amplification of

362   fragments used in construct design was carried out using Phusion® high fidelity DNA polymerase (NEB).

363

Indirect immunofluorescence Analysis (IFA) and Western blots

365   For IFA, thin blood films were prepared from synchronous *P. falciparum* cultures enriched in

366   mature schizonts. The air-dried thin films were fixed in 4% (w/v) paraformaldehyde for 30 min,

367   permeabilised with 0.1% (v/v) Triton X-100 for 10 min, and blocked overnight in 3% (w/v) bovine serum

368   albumin (BSA) in PBS. Slides were probed with rat anti-HA 3F10 (1:100) to detect HA-tagged proteins,

369   human anti-MSP1 monoclonal antibody (mAb) X509 (1:500) to detect MSP1, mAb 89 (1:100) to detect

370   KAHRP, and mAb 2G12 (1:100) to detect HRP2. Primary antibodies were detected using Alexa Fluor

371   594-conjugated anti-human or anti-mouse secondary antibodies (Life Technologies), and Alexa Fluor

372   488-conjugated streptavidin (Life Technologies), diluted 1:2000. Slides were stained with 4,6-diamidino-

373   2-phenylindole (DAPI), mounted in Citifluor (Citifluor Ltd., UK). Images were visualised using a Nikon

374   Eclipse Ni microscope with LED-illumination with a 63x Plan Apo λ NA 1.4 objective. Images were

17

375 taken using an Orca Flash 4 digital camera controlled by Nikon NIS Element AR 4.30.02 software. All

376 images were subsequently analysed using FIJI software.

377 For Western blots, Percoll-enriched schizonts were pelleted, then resuspended into 10 volumes of

378 PBS. Samples were solubilised into SDS sample buffer, boiled, sonicated and centrifuged. The extracts

379 were subjected to SDS-PAGE under reducing conditions followed by transfer to nitrocellulose

380 membrane. Membranes were probed with rat anti-HA 3F10 (1:1000), human anti-MSP1 mAb X509

381 (1:1000), anti-GFP (1:1000), mAb 89 (1:1000) or mAb 2G12 (1:1000), followed by horseradish

382 peroxidase-conjugated secondary antibodies. Antigen-antibody interactions were visualised by enhanced

383 chemiluminescence (SuperSignal West Pico chemiluminescent substrate, Pierce).

384

Parasite growth assay

386 Parasitaemia measurement by FACS was as described previously [43]. Briefly, parasites

387 recovered at various time-points were fixed in 8% paraformaldehyde 0.04% glutaraldehyde, pH 7.4 and

388 stained with 2 µM Hoechst 33342 (Invitrogen, Waltham, MA). Parasitaemia was calculated using the

389 FACS BD Fortessa flow cytometer (BD Biosciences). Briefly, cultures to be analysed were initially

390 screened using forward and side scatter parameters and gated for erythrocytes. From this gated

391 population, the proportion of Hoechst-stained cells in 100,000 cells was determined using ultraviolet light

392 with a violet filter (450/50 nm). Samples were analysed using FlowJo software.

393

18

Acknowledgements

Author Contributions

Conceived and designed the experiments: NB, CRC, FH, CWM, MJB. Performed the experiments: NB, CRC, FH. Analysed the data: NB, CRC, MJB. Wrote the paper: NB, CRC, MJB.

References
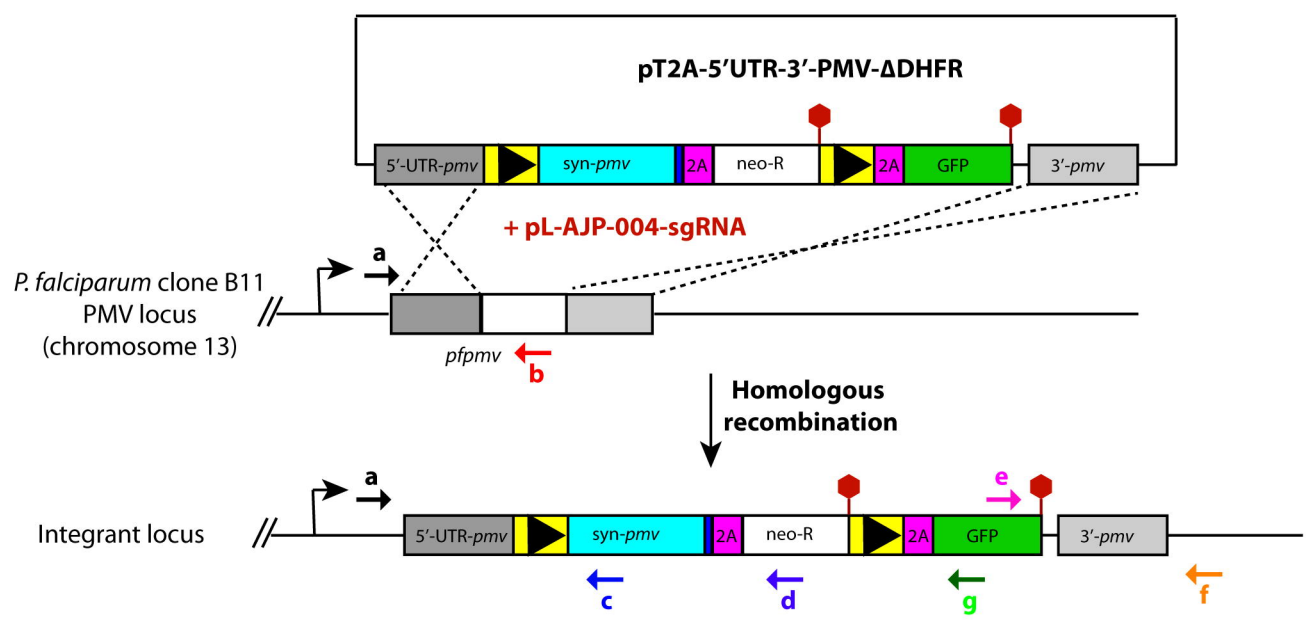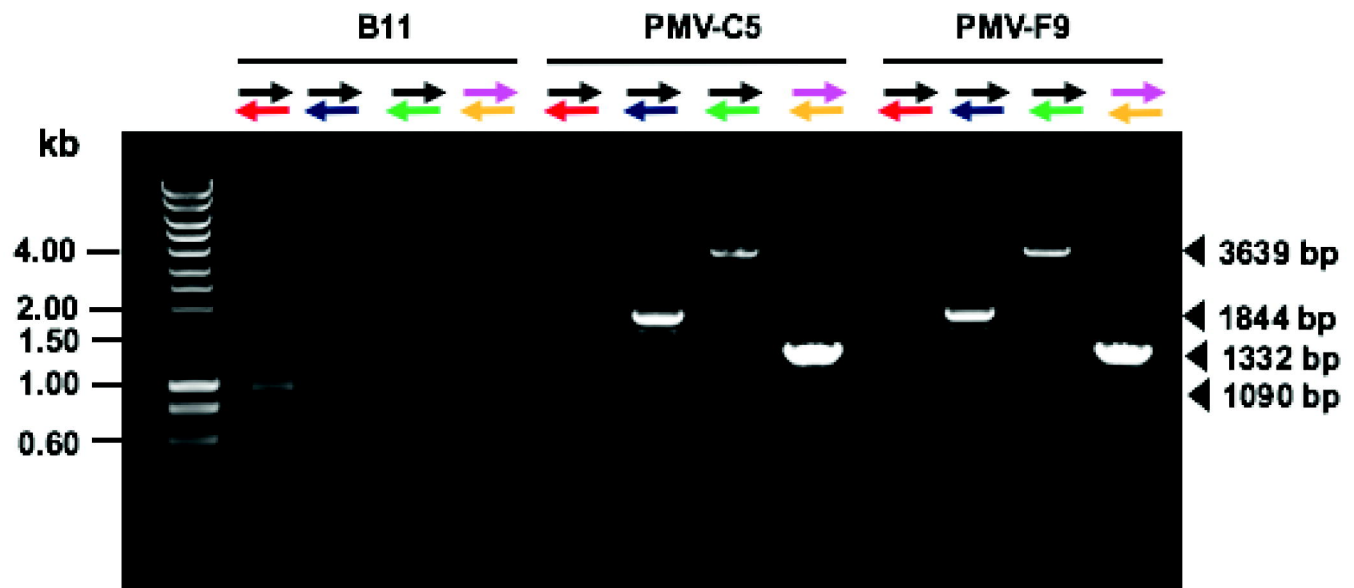
1. WHO. World Malaria Report (2017).

2. Haase S, de Koning-Ward TF. New insights into protein export in malaria parasites. Cell Microbiol. (2010);12: 580-587.

3. Boddey JA, Cowman AF. *Plasmodium* nesting: remaking the erythrocyte from the inside out. Annu Rev Microbiol. (2013);67: 243-269.

4. de Koning-Ward TF, Gilson PR, Boddey JA, Rug M, Smith BJ, et al. A newly discovered protein export machine in malaria parasites. Nature. (2009);459: 945-949.

5. Bullen HE, Charnaud SC, Kalanon M, Riglar DT, Dekiwadia C, et al. Biosynthesis, localization, and macromolecular arrangement of the *Plasmodium falciparum* translocon of exported proteins (PTEX). J Biol Chem. (2012); 287: 7871-7884.

6. Maier AG, Rug M, O'Neill MT, Brown M, Chakravorty S, et al. Exported proteins required for virulence and rigidity of *Plasmodium falciparum*-infected human erythrocytes. Cell. (2008);134: 48-61.

7. Elsworth B, Crabb BS, Gilson PR. Protein export in malaria parasites: an update. Cell Microbiol. (2014);16: 355-363.

8. Spillman NJ, Beck JR, Goldberg DE. Protein export into malaria parasite-infected erythrocytes: mechanisms and functional consequences. Annu Rev Biochem. (2015);84: 813-841.

9. Hiller NL, Bhattacharjee S, van Ooij C, Liolios K, Harrison T, et al. A host-targeting signal in virulence proteins reveals a secretome in malarial infection. Science. (2004);306: 1934-1937.

10. Marti M, Good RT, Rug M, Knuepfer E, Cowman AF. Targeting malaria virulence and remodeling proteins to the host erythrocyte. Science. (2004);306: 1930-1933.
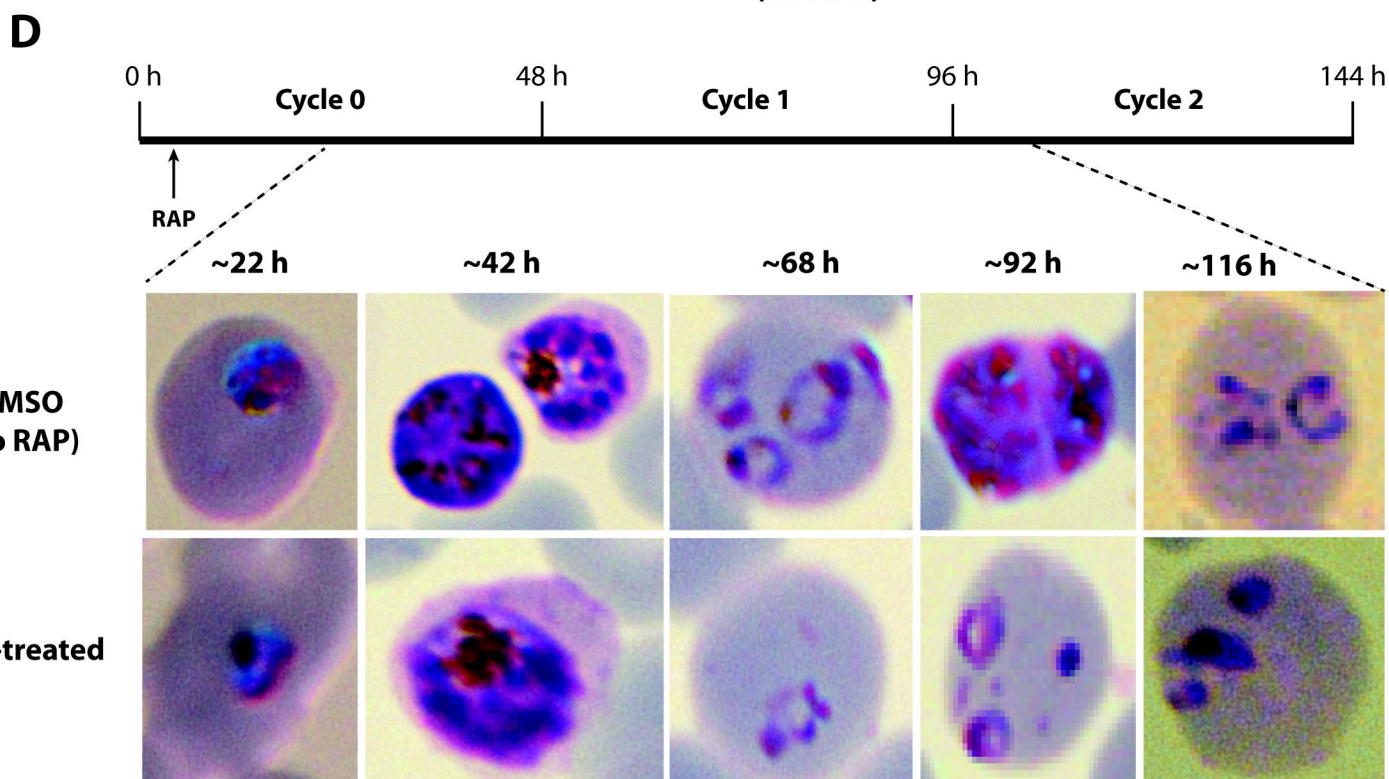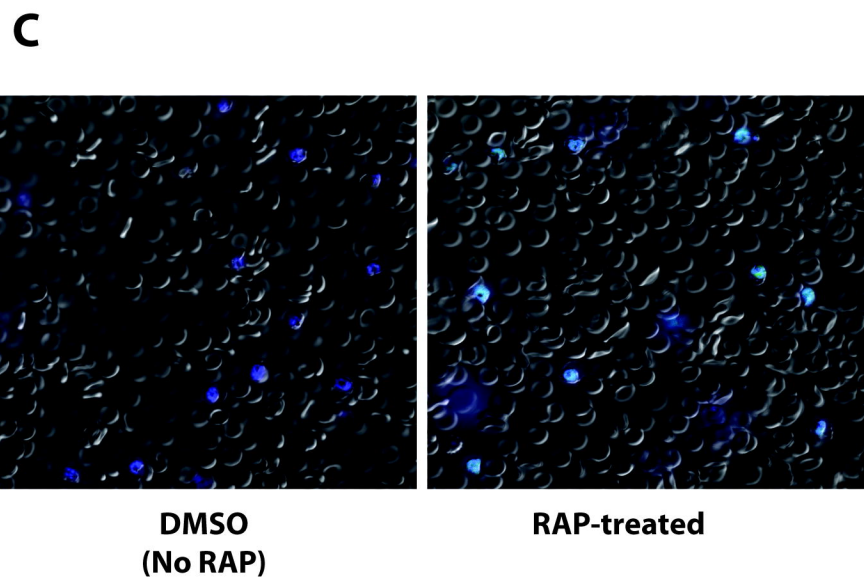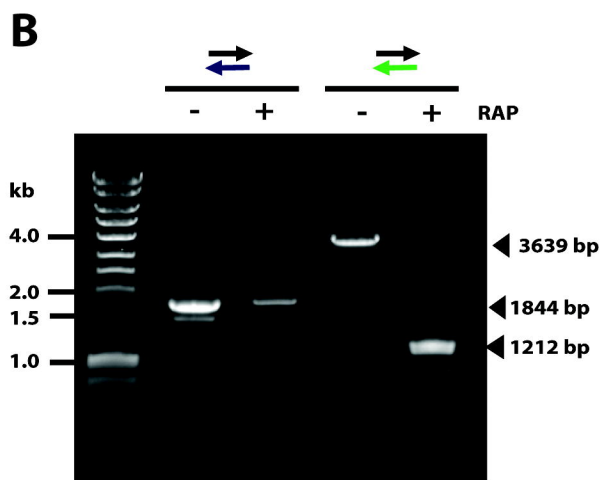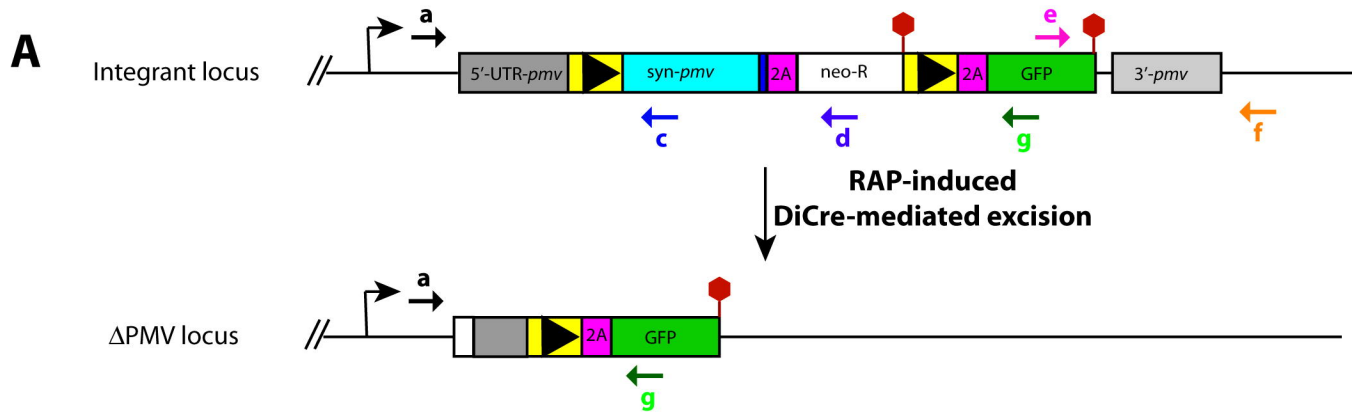
426   11. Spielmann T, Gilberger TW. Protein export in malaria parasites: do multiple export motifs add up to

427   multiple export pathways? Trends Parasitol. (2010);26: 6-10.

428   12. Heiber A, Kruse F, Pick C, Gruring C, Flemming S, et al. Identification of new PNEPs indicates a

429   substantial non-PEXEL exportome and underpins common features in *Plasmodium falciparum* protein

430   export. PLoS Pathog. (2013);9: e1003546.

431   13. Klemba M, Goldberg DE. Characterization of plasmepsin V, a membrane-bound aspartic protease

432   homolog in the endoplasmic reticulum of *Plasmodium falciparum*. Mol Biochem Parasitol.

433   (2005);143: 183-191.

434   14. Gruring C, Heiber A, Kruse F, Flemming S, Franci G, et al. Uncovering common principles in protein

435   export of malaria parasites. Cell Host Microbe. (2012);12: 717-729.

436   15. Hodder AN, Sleebs BE, Czabotar PE, Gazdik M, Xu Y, et al. Structural basis for plasmepsin V

437   inhibition that blocks export of malaria proteins to human erythrocytes. Nat Struct Mol Biol.

438   (2015);22: 590-596.

439   16. Sleebs BE, Gazdik M, O'Neill MT, Rajasekaran P, Lopaticki S, et al. Transition state mimetics of the

440   Plasmodium export element are potent inhibitors of Plasmepsin V from *P. falciparum* and *P. vivax*. J

441   Med Chem. (2014);57: 7644-7662.

442   17. Gambini L, Rizzi L, Pedretti A, Taglialatela-Scafati O, Carucci M, et al. Picomolar Inhibition of

443   Plasmepsin V, an Essential Malaria Protease, Achieved Exploiting the Prime Region. PLoS One.

444   (2015);10: e0142509.

445   18. Sleebs BE, Lopaticki S, Marapana DS, O'Neill MT, Rajasekaran P, et al. Inhibition of Plasmepsin V

446   activity demonstrates its essential role in protein export, *Pf*EMP1 display, and survival of malaria

447   parasites. PLoS Biol. (2014);12: e1001897.

448   19. Goldberg DE. Plasmepsin V shows its carnivorous side. Nat Struct Mol Biol. (2015);22: 647-648.
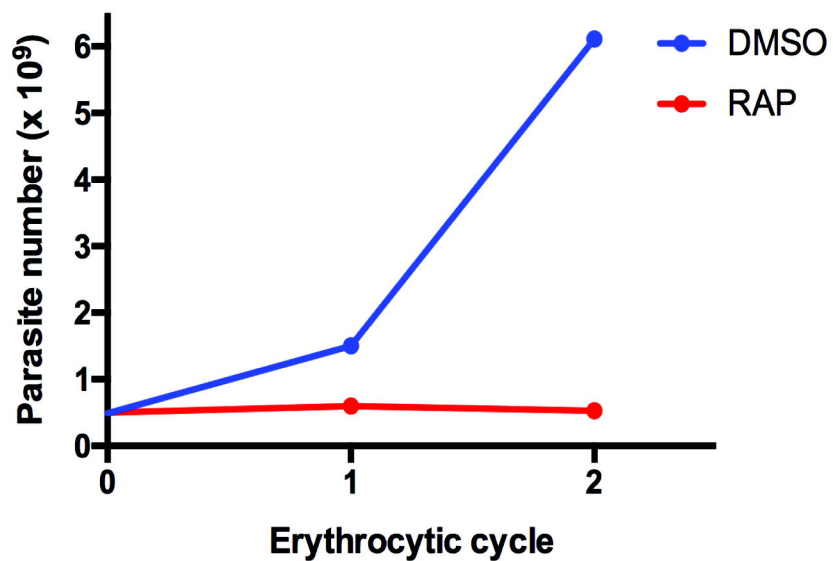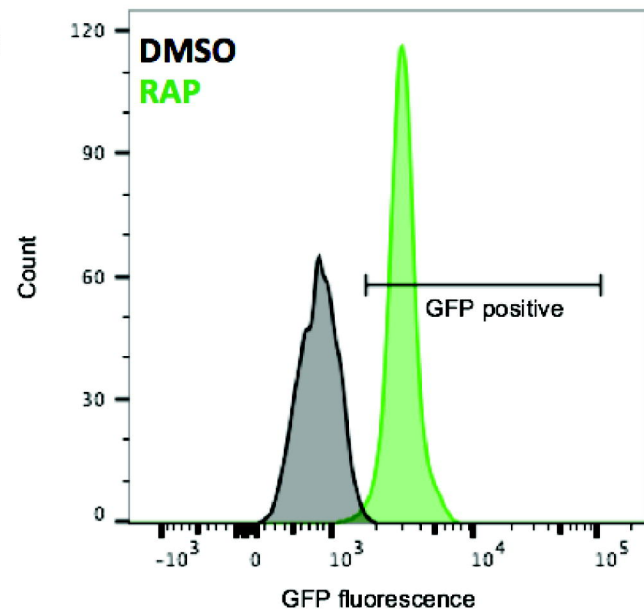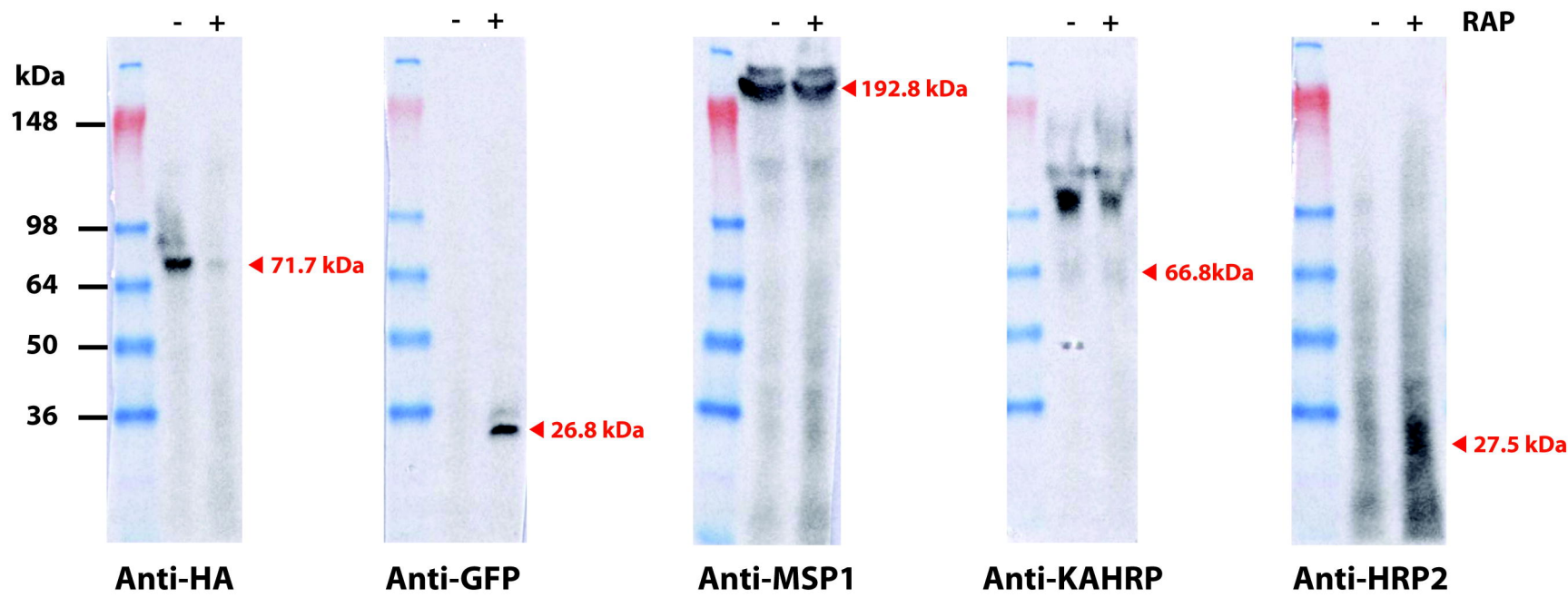
449   20. Boddey JA, Hodder AN, Gunther S, Gilson PR, Patsiouras H, et al. An aspartyl protease directs

450   malaria effector proteins to the host cell. Nature. (2010);463: 627-631.

451   21. Russo I, Babbitt S, Muralidharan V, Butler T, Oksman A, et al. Plasmepsin V licenses *Plasmodium*

452   proteins for export into the host erythrocyte. Nature. (2010);463: 632-636.

453   22. Collins CR, Das S, Wong EH, Andenmatten N, Stallmach R, et al. Robust inducible Cre recombinase

454   activity in the human malaria parasite *Plasmodium falciparum* enables efficient gene deletion within a

455   single asexual erythrocytic growth cycle. Mol Microbiol. (2013);88: 687-701.

456   23. Ghorbal M, Gorman M, Macpherson CR, Martins RM, Scherf A, et al. Genome editing in the human

457   malaria parasite *Plasmodium falciparum* using the CRISPR-Cas9 system. Nat Biotechnol. (2014);32:

458   819-821.

459   24. Jones ML, Das S, Belda H, Collins CR, Blackman MJ, et al. A versatile strategy for rapid conditional

460   genome engineering using loxP sites in a small synthetic intron in *Plasmodium falciparum*. Sci Rep.

461   (2016);6: 21800.

462   25. Birnbaum J, Flemming S, Reichard N, Soares AB, Mesen-Ramirez P, et al. A genetic system to study

463   *Plasmodium falciparum* protein function. Nat Methods. (2017);14: 450-456.

464   26. Perrin AJ, Collins, C.R., Russell, M.R.G., Collinson, L.M., Baker, D.A., Blackman, M.J.

465   Actinomyosin-Based Motility Drives Malaria Parasite Red Blood Cell Invasion but not Egress.

466   (submitted for publication).

467   27. Das S, Hertrich N, Perrin AJ, Withers-Martinez C, Collins CR, et al. Processing of *Plasmodium*

468   *falciparum* Merozoite Surface Protein MSP1 Activates a Spectrin-Binding Function Enabling Parasite

469   Egress from RBCs. Cell Host Microbe. (2015);18: 433-444.

470   28. Boddey JA, Carvalho TG, Hodder AN, Sargeant TJ, Sleebs BE, et al. Role of plasmepsin V in export

471   of diverse protein families from the *Plasmodium falciparum* exportome. Traffic. (2013);14: 532-550.
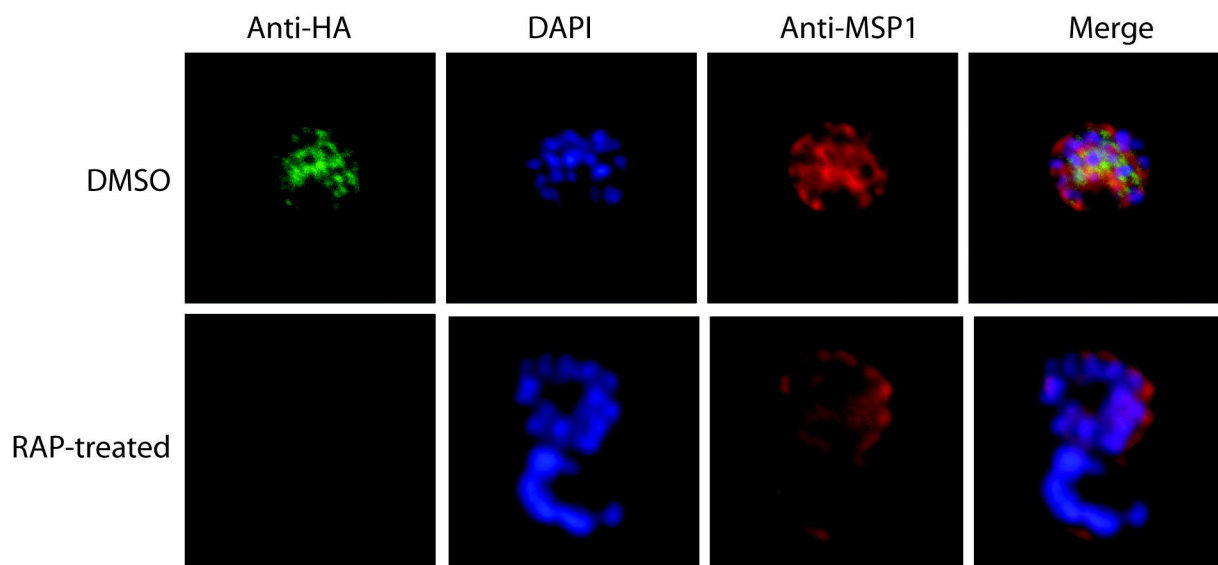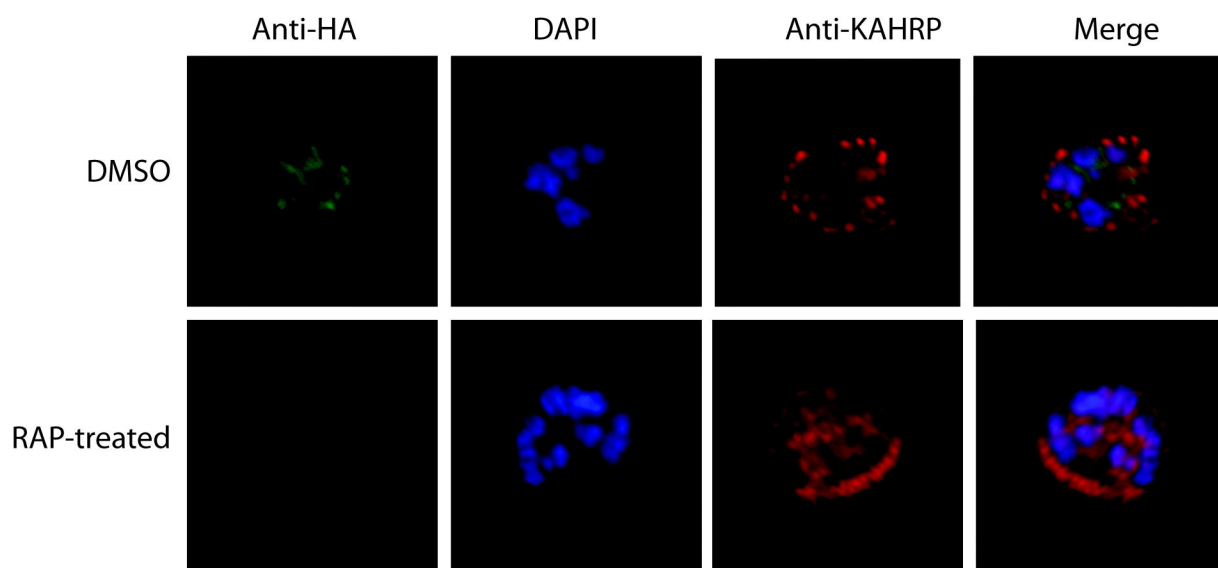
472   29. Collins CR, Hackett F, Atid J, Tan MSY, Blackman MJ. The *Plasmodium falciparum* pseudoprotease

473   SERA5 regulates the kinetics and efficiency of malaria parasite egress from host erythrocytes. PLoS

474   Pathog. (2017);13: e1006453.

475   30. Sherling ES, Knuepfer E, Brzostowski JA, Miller LH, Blackman MJ, et al. The *Plasmodium*

476   *falciparum* rhoptry protein RhopH3 plays essential roles in host cell invasion and nutrient uptake.

477   Elife. (2017); 6.

478   31. Szymczak AL, Workman CJ, Wang Y, Vignali KM, Dilioglou S, et al. Correction of multi-gene

479   deficiency in vivo using a single 'self-cleaving' 2A peptide-based retroviral vector. Nat Biotechnol.

480   (2004);22: 589-594.

481   32. Straimer J, Lee MC, Lee AH, Zeitler B, Williams AE, et al. Site-specific genome editing in

482   *Plasmodium falciparum* using engineered zinc-finger nucleases. Nat Methods. (2012);9: 993-998.

483   33. Beck JR, Muralidharan V, Oksman A, Goldberg DE. PTEX component HSP101 mediates export of

484   diverse malaria effectors into host erythrocytes. Nature. (2014);511: 592-595.

485   34. Elsworth B, Matthews K, Nie CQ, Kalanon M, Charnaud SC, et al. PTEX is an essential nexus for

486   protein export in malaria parasites. Nature. (2014);511: 587-591.

487   35. Trager W, Jensen JB. Human malaria parasites in continuous culture. Science. (1976);193: 673-675.

488   36. Blackman MJ. Purification of *Plasmodium falciparum* merozoites for analysis of the processing of

489   merozoite surface protein-1. Methods Cell Biol. (1994);45: 213-220.

490   37. Saul A, Myler P, Elliott T, Kidson C. Purification of mature schizonts of *Plasmodium falciparum* on

491   colloidal silica gradients. Bull World Health Organ. (1982);60: 755-759.

492   38. Harris PK, Yeoh S, Dluzewski AR, O'Donnell RA, Withers-Martinez C, et al. Molecular

493   identification of a malaria merozoite surface sheddase. PLoS Pathog. (2005);1: 241-251.

494   39. Lambros C, Vanderberg JP. Synchronization of Plasmodium falciparum erythrocytic stages in culture.

495   J Parasitol. (1979);65: 418-420.

496   40. Ryan MD, King AM, Thomas GP. Cleavage of foot-and-mouth disease virus polyprotein is mediated

497   by residues located within a 19 amino acid sequence. J Gen Virol. (1991);72 (Pt 11): 2727-2732.

498   41. Knuepfer E, Napiorkowska M, van Ooij C, Holder AA. Generating conditional gene knockouts in

499   *Plasmodium* - a toolkit to produce stable DiCre recombinase-expressing parasite lines using

500   CRISPR/Cas9. Sci Rep. (2017);7: 3881.

501   42. Thomas JA, Collins CR, Das S, Hackett F, Graindorge A, et al. Development and Application of a

502   Simple Plaque Assay for the Human Malaria Parasite *Plasmodium falciparum*. PLoS One. (2016);11:

503   e0157873.

504   43. Stallmach R, Kavishwar M, Withers-Martinez C, Hackett F, Collins CR, et al. *Plasmodium*

505   *falciparum* SERA5 plays a non-enzymatic role in the malarial asexual blood-stage lifecycle. Mol

506   Microbiol. (2015);96: 368-387.

A

pT2A-5'UTR-3'-PMV-ΔDHFR

5'-UTR-*pmv* | syn-*pmv* | 2A | neo-R | 2A | GFP | 3'-*pmv*

+ pL-AJP-004-sgRNA

P. falciparum clone B11
PMV locus
(chromosome 13)

a

pfpmv

b

Homologous recombination

Integrant locus

a

5'-UTR-*pmv* | syn-*pmv* | 2A | neo-R | 2A | GFP | 3'-*pmv*

c   d   g   f

e

B

kb

B11   PMV-C5   PMV-F9

4.00 — ◄ 3639 bp

2.00 — ◄ 1844 bp
1.50 — ◄ 1332 bp

1.00 — ◄ 1090 bp

0.60 —

A Integrant locus

a

5'-UTR-*pmv* syn-*pmv* 2A neo-R 2A GFP 3'-*pmv*

c d e g f

RAP-induced
DiCre-mediated excision

ΔPMV locus

a

2A GFP

g

B

kb

4.0 ◄ 3639 bp

2.0 ◄ 1844 bp
1.5

1.0 ◄ 1212 bp

− + RAP − +

C

DMSO
(No RAP)

RAP-treated

D

0 h   48 h   96 h   144 h

Cycle 0   Cycle 1   Cycle 2

RAP

~22 h   ~42 h   ~68 h   ~92 h   ~116 h

DMSO
(no RAP)

RAP-treated

A

Parasite number (x 10^9) vs Erythrocytic cycle

DMSO
RAP

B

DMSO
RAP

Count vs GFP fluorescence

GFP positive

C

kDa

148

98

64

50

36

◄ 71.7 kDa

◄ 26.8 kDa

◄ 192.8 kDa

◄ 66.8kDa

◄ 27.5 kDa

RAP

Anti-HA   Anti-GFP   Anti-MSP1   Anti-KAHRP   Anti-HRP2

A

	Anti-HA	DAPI	Anti-MSP1	Merge
DMSO				
RAP-treated				

B

	Anti-HA	DAPI	Anti-KAHRP	Merge
DMSO				
RAP-treated				

C

	Anti-HA	DAPI	Anti-HRP2	Merge
DMSO				
RAP-treated				